

Self-Phase Modulation and "Rocking" of Molecules in Trapped Filaments of Light with Picosecond Pulses*

R. Cubeddu, R. Polloni, C. A. Sacchi, and O. Svelto

*Gruppo di Elettronica Quantistica del Consiglio Nazionale delle Ricerche,
Istituto di Fisica del Politecnico, Milano, Italy*

(Received 19 January 1970)

The spectral properties of trapped filaments of light in many liquids have been studied in detail using, as an excitation source, a ruby laser operating in different regimes. It has been found that the regular periodic structures in the spectra, which are typical of the self-phase modulation process, can be obtained with high reproducibility under excitation with laser pulses of ≈ 5 psec. These properties have been interpreted using the method of stationary phase, which makes it possible to derive the temporal behavior of the nonlinear refractive index δn in the filaments in a fairly simple way. Other conclusions deduced from this method about the structure of the spectra have been confirmed by experiment. By using a functional relation between δn and the optical field intensity A^2 based on a model given by Starunov the relaxation time τ_1 of δn and the temporal behavior of the pulse intensity have also been derived. The value of τ_1 , which is consistently of the order of a few tenths of a picosecond, gives a strong indication that a "molecular rocking" is the main mechanism for trapping with picosecond excitation. The optical pulse derived has a time width of ≈ 2.5 psec and an asymmetrical shape. The self-consistency of the method employed has been checked by using the derived pulses $\delta n(t)$ and $A(t)$ to calculate, by computer, the spectral power density of the optical pulse. The spectrum so calculated fits the experimental one fairly well.

I. INTRODUCTION

The self-trapping of intense laser beams in liquids has been studied by several authors over the last few years. Particular attention has been devoted both to the physical mechanisms which may be responsible for the formation of small-scale filaments and to the nonlinearities which occur in the filaments owing to the extremely high electric field. Self-trapped filaments have been observed with different excitations. In the most studied case, when a Q -switched laser pulse with a few tens of nanoseconds' duration has been used as the excitation source, the molecular orientational Kerr effect has been considered to be the most important mechanism for filament formation.¹

Among the physical properties of trapped light, the spectral composition is perhaps the most striking. Under Q -switched single-mode excitation, evidence of large broadening with occasional periodic structures in the spectra of the filaments was first reported by Grieneisen and Sacchi, and Brewer.² Regular and peculiar spectral structures obtained by Shimizu,³ under Q -switched, yet multi-mode, laser operation have been interpreted in terms of self-phase modulation of a trapped optical pulse. A more complete treatment of the self-modulation process has been given by Gustafson *et al.*,⁴ who have pointed out the importance of a pulse shortening of the laser excitation in order to have agreement with the experimental spectra. A possible process of short-pulse formation has

been described by Marburger *et al.*⁵ in a treatment of self-focusing in a transient regime. Self-modulation of a sinusoidal modulation of laser intensity induced by a process within the liquid suggested by Cheung *et al.*⁶ can equally well fit the experimental spectra when a fine structure⁷ is observed. Finally, ultrashort pulses of a mode-locked laser have been used for a trapping experiment by Brewer and Lee.⁸ These last authors, who did not report spectral observations of the trapped light, introduced a molecular electronic distortion as the main mechanism for trapping formation in the case of picosecond excitation.

A previous work⁹ reported the observation of very regular and reproducible spectra of trapped filaments under picosecond excitation, and it has been suggested that a fast mechanism ("rocking" of molecules in a potential well) could be the most important mechanism in ultrashort excitation.

The purposes of this work are (i) to report on experimental results which confirm the importance of short laser pulses to obtain broad and regular spectra of trapped light and (ii) to describe a treatment, based on the model of molecular rocking and on the method of stationary phase, which allows the measurement of important physical parameters of the trapping mechanism.

II. EXPERIMENTAL RESULTS

On studying the spectral properties of the filaments, the excitation source used was a ruby laser operating in three different regimes: (i) Q -switched with a single transverse and longitudinal mode,

(ii) mode-locked, with a single transverse mode and a pulse width of ≈ 1 nsec, and (iii) mode-locked, with a single transverse mode giving ultrashort pulses (20–5 psec). These types of lasers have been described in previous works.^{10–12} The experimental apparatus is very similar to that used in this kind of experiment by other authors.^{2,3} Some of the usual liquids (CS_2 , toluene, bromobenzene) have been tested, in cells of different lengths (5–25 cm).

In the first series of experiments, a single-transverse (TEM_{00}) longitudinal-mode Q -switched ruby laser, giving a pulse ≈ 30 nsec in duration and a peak power density up to 100 Mw/cm^2 , was used. In this case, a plane or slightly converging input beam produced a single filament most of the time, provided that the laser power was kept below twice the focusing threshold. The results on spectral broadening, however, were found to depend on the distance of the liquid cell from the laser. Let us consider the two following cases. (i) Case of small distances (<1 m): A plane or slightly converging beam produced an intense laser component and relevant Raman content at the first and second Stokes lines. The broadening of these lines spanned several tens to several hundreds of cm^{-1} (depending on the laser power), the spectra exhibiting discrete but rather irregular structures. If the input beam was strongly focused inside the liquid, a more intense and broad spectrum of the filaments was obtained with an enhancement of Raman radiation and the appearance of more regular discrete patterns in the spectra. (ii) If the liquid cell was moved a few meters away from the laser, the frequency broadening of the filaments was strongly reduced, becoming of the order of a few cm^{-1} . This result was found to hold substantially for both focused and unfocused beams. These observations are in agreement with the possibility that short pulses are of importance in producing a more or less regular broad spectrum.⁴ Indeed, in spite of the single-mode character of our input beam, short pulses may be produced in the back-scattered Brillouin radiation,¹³ which enters the liquid cell after being reamplified in the laser cavity.¹⁴

To check this possibility, a mode-locked ruby laser with a single-transverse mode (TEM_{00}) and a pulse duration ≈ 1 nsec was used as an excitation source. With such short pulses, it is well known¹⁵ that the Brillouin effect is strongly reduced. In this case, a plane beam entering the liquid cell produced many filaments with a rather narrow spectrum, spanning only a few cm^{-1} , independent of the distance of the liquid from the laser. This confirms the importance of Brillouin scattering to produce, even in an indirect way, frequency broadening of the filaments, and it indicates that our

pulses were not short enough to produce large frequency broadening.

A third experiment employed a TEM_{00} -mode mode-locked ruby laser, generating ultrashort pulses in the range 20–5 psec, according to the dye used,¹¹ and a power density $\approx 5 \text{ Gw/cm}^2$. No lenses were put in front of the liquid cell, and the immediate appearance of broad highly regular spectra of the type reproduced in Fig. 1 was observed. In the case of the shortest excitation, this kind of spectrum is exhibited by each filament in a very reproducible way. The spectra may span a few tens to several hundreds of cm^{-1} , depending on the laser power, and extend both to the Stokes and to the anti-Stokes side. The Stokes component is, however, more intense. Almost no Raman light was present in the case of CS_2 .

The main fact that can be deduced from these results is that the very regular and characteristic spectra, which have been attributed to self-modulation, are mainly due to self-focusing of ultrashort pulses, which directly enter the liquid or are produced in different nonlinear processes, like the Brillouin scattering or the self-focusing itself.⁵ It is likely that short pulses were present (even if not explicitly verified) in the multimode Q -switched excitation used by other authors, who obtained regular spectra.

It is worth noting that in the case of picosecond excitation, a fine structure⁷ with a period ranging 7–10 cm^{-1} was occasionally observed in all the previous liquids. Since the spectra that exhibit fine structure are among the broadest and most intense ones, it is likely that the modulation process responsible for this effect is produced in the filaments (where there are the strongest fields) rather than being present at the initiation of all the filaments.

Finally, measurements of filament diameters, although not extensively performed for all the

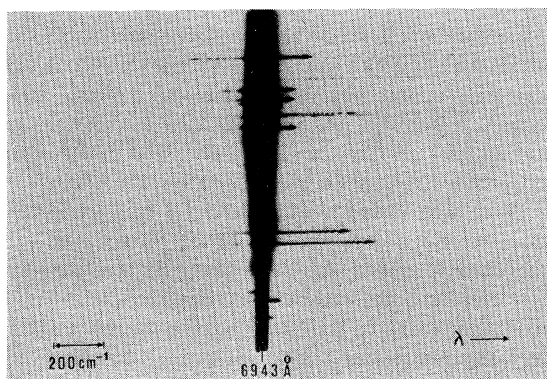


FIG. 1. Typical regular spectra due to self-phase modulation as obtained with picosecond excitation.

liquids, gave a value $\approx 5 \mu$ for CS_2 , with both nano-second and picosecond excitation. Since, in the latter case, the Brillouin and Raman effects are almost absent, it may be concluded that they do not play an important role in diameter stabilization.

III. INTERPRETATION OF THE SPECTRA

According to what has been done elsewhere,^{3, 4, 9} the spectrum $f(z, \omega)$ of the light pulse after traveling a distance z in the filament can be written as

$$f(z, \omega) = e^{ikz} \int_{-\infty}^{\infty} A(t, z) e^{i(\gamma \delta n + \omega t)} dt, \quad (1)$$

where $A(t, z)$ is the field amplitude $\gamma = \omega_0 z / c$, δn is the nonlinear refractive index induced by the field, ω_0 is the laser angular frequency, and ω is the angular frequency of the spectrum minus ω_0 . As done by Gustafson *et al.*,⁴ one can assume a given shape for $A(t, z)$ and a given functional relation between δn and A , and then, by computer, calculate $f(z, \omega)$ to fit the experimental results. Interesting pieces of information can, however, be obtained by approximately calculating the integral in Eq. (1) by the method of stationary phase.¹⁶ This method makes use of the intuitive observation that, at each angular frequency ω , the main contribution to the integral (1) comes from the points at which

$$\gamma \frac{d\delta n}{dt} = -\omega. \quad (2)$$

Now, this method provides for an asymptotic expansion of the integral (1) which holds when $\gamma \rightarrow \infty$. The results which follow are, therefore, believed to hold with greater accuracy for the widest observed spectra.

For what follows, the following assumptions will be made. (a) The spectral broadening of the function $f(z, \omega)$ is mainly due to the phase term $e^{i(\gamma \delta n + \omega t)}$ rather than to the amplitude term $A(t, z)$ appearing in Eq. (1). (b) The curve describing $\delta n = \delta n(t)$ has a bell-shaped, but not necessarily symmetrical, form. On the above two assumptions, it will be shown that from the observed spectra one can almost completely reconstruct the function $\gamma \delta n(t)$. In order to know the absolute value of $\delta n(t)$, one should know the value of γ , i.e., the value of the propagation distance z of the filament in the liquid. This can be done experimentally by using pin-hole techniques, as done by Denariez and Taran.¹⁷ It has not, however, been done in our experiments, so that the absolute value of $\delta n(t)$ will be inferred from the measured filament diameter.

For what follows reference will be made to Fig. 2, where a typical spectrum is shown schematically

[Fig. 2(a)] and a bell-shaped curve is assumed for $\delta n(t)$ [Fig. 2(b)]. In Fig. 2(b), the two inflection points 1 and 2 and the peak value of δn are also indicated. It will be shown that, by using the method of stationary phase, the following quantities are easily obtained from the spectra: (i) $\gamma \delta n_1$ and $\gamma \delta n_2$, (ii) $\gamma(d\delta n/dt)_1$ and $\gamma(d\delta n/dt)_2$, (iii) $\gamma(d^3\delta n/dt^3)_1$ and $\gamma(d^3\delta n/dt^3)_2$, and (iv) $\gamma \delta n_p$, where the subscripts 1 and 2 refer to the inflection points. Measurement of the above quantities makes it possible to determine a power expansion of $\gamma \delta n(t)$ up to the third order, which provides a fairly accurate description of the function in a wide range around the peak value.

The calculation of the first time derivatives at the inflection points comes immediately from Eq. (2). Indeed, we have

$$\gamma \left(\frac{d\delta n}{dt} \right)_1 = -\omega_s, \quad (3a)$$

$$\gamma \left(\frac{d\delta n}{dt} \right)_2 = -\omega_{as}, \quad (3b)$$

where $\omega_s = 2\pi\nu_s$ and $\omega_{as} = 2\pi\nu_{as}$ are the extensions of the spectra at the Stokes and anti-Stokes side, respectively [see Fig. 2(a)]. It is immediately obvious that, if the two extensions are not equal, the curve $\delta n(t)$ will not be symmetrical.

To calculate $\gamma \delta n_p$, let us first consider a given frequency ω at the Stokes side ($|\omega| < |\omega_s|$). According to Eq. (2), the main contributions to the integral (1) come from the two points t' and t'' [Fig. 2(b)] at which

$$\gamma \left(\frac{d\delta n}{dt} \right)_{t=t'} = \gamma \left(\frac{d\delta n}{dt} \right)_{t=t''} = -\omega. \quad (4)$$

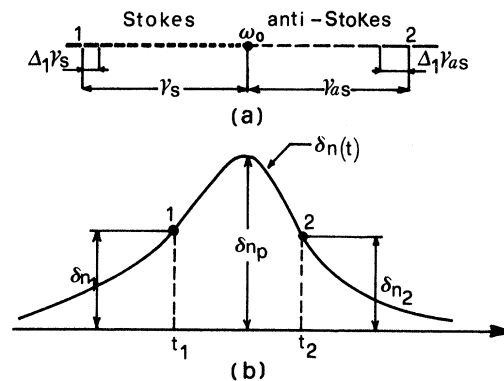


FIG. 2. (a) Schematic drawing of a typical spectrum. (b) Bell-shaped curve (not necessarily symmetrical) which is assumed for the nonlinear refractive index $\delta n(t)$ and which is used in discussion of the text.

The method of stationary phase then gives, for $f(z, \omega)$,

$$f(z, \omega) = \left(\frac{4\pi}{\gamma}\right)^{1/2} e^{i(kz - \pi/2)} \left(\frac{A(t') e^{i[\gamma\delta n(t') + \omega t']}}{(d^2\delta n/dt^2)_{t=t'}}^{1/2} + \frac{A(t'') e^{i[\gamma\delta n(t'') + \omega t'']}}{(d^2\delta n/dt^2)_{t=t''}}^{1/2} \right). \quad (5)$$

It is immediately evident from Eq. (5) that $|f(z, \omega)|^2$ will be at a minimum when

$$\gamma\delta n(t') + \omega t' = \gamma\delta n(t'') + \omega t'' + (2l - 1)\pi, \quad (6)$$

where l is an integer ($l = 1, 2, \dots$). Equation (6) is easily understood from a physical point of view; it simply states that in order to have a minimum in the spectrum the contributions from the two points t' and t'' must be 180° out of phase, so that they will cancel each other out by interference. Let us now consider Eq. (6) at the particular frequency $\omega = 0$ (i. e., the laser frequency). From Eq. (4) and Fig. 2(b), we then have $t' = t_p$, $t'' \rightarrow -\infty$, $\delta n(t') = \delta n_p$, and $\delta n(t'') = 0$. We now further assume that $\omega t'' = -\gamma t'' (d\delta n/dt)_{t=t''} \rightarrow 0$ when $t'' \rightarrow -\infty$, which implies that $\delta n(t)$ must go to 0 at infinity at least as fast as $1/t^\alpha$ with α positive. From this assumption, one gets from Eq. (6) for $\omega = 0$

$$\gamma\delta n_p = (2m - 1)\pi, \quad (7)$$

where m is the total number of minima of the spectrum at the Stokes side. Equation (7) readily gives $\gamma\delta n_p$ once m has been measured from the spectrum. Taking into account the expression for γ , Eq. (7) can be put in the form $\delta n_p = (2m - 1)\lambda_0/2z \approx m\lambda_0/z$, which relates the peak value of δn to the central wavelength λ_0 and to the number of sidebands per unit length m/z generated in the liquid. Since the previous calculation can equally well be applied to a frequency ω at the anti-Stokes side, we also come to the conclusion that the number of minima m of the spectrum at the Stokes side is equal to that at the anti-Stokes side. This result is somewhat intuitive, since it simply states that the number of sidebands due to the phase-modulation process is equal at both the Stokes and the anti-Stokes side. It is also a very useful result, since the observed anti-Stokes spectrum is sometimes very weak, so that the number of minima there cannot be easily measured.

It is important to note that Eq. (5) is not valid for $\omega = \omega_S$ (and $\omega = \omega_{aS}$), i. e., at the frequency extrema of the spectrum. Indeed, when $\omega = \omega_S$, the main contribution to the integral (1) will come from the point $t = t_1$, where $(d^2\delta n/dt^2)_1 = 0$. In this case, the method of stationary phase gives the following result for $f(\omega_S, z)$:

$$f(\omega_S, z) = [6^{1/3} \Gamma(\frac{4}{3}) e^{ikz} e^{i(\gamma\delta n_1 + \omega_S t_1 + \pi/6)}] \times A(t_1) \left/ \left(\gamma \frac{d^3\delta n}{dt^3} \right)_1 \right.^{1/3}. \quad (8)$$

The corresponding result at $\omega = \omega_{aS}$ can be readily obtained from Eq. (8) by substituting the subscript 2 for the subscript 1 and ω_{aS} for ω_S . The result shown in Eq. (8) comes from a power-series expansion up to the third order of the function $\gamma\delta n(t)$ around the point $t = t_1$, namely,

$$\gamma\delta n = \gamma\delta n_1 - \omega_S(t - t_1) + \frac{1}{6} \left(\gamma \frac{d^3\delta n}{dt^3} \right)_1 (t - t_1)^3, \quad (9)$$

where use has been made of Eq. (3a).

To calculate $(\gamma d^3\delta n/dt^3)_1$, we have to consider the integral (1) at frequency $\omega \approx \omega_S$ [a similar calculation at frequency $\omega \approx \omega_{aS}$ produces the expression $(\gamma d^3\delta n/dt^3)_2$]. When ω is sufficiently close to ω_S , the power expansion (9) holds for $\gamma\delta n$ so that, according to Eq. (2), the main contributions to the integral (1) will come from the two points t_\pm given by the equation

$$(t_\pm - t_1) = \pm \left[2\Delta\omega_S / \left(\gamma \frac{d^3\delta n}{dt^3} \right)_1 \right]^{1/2}, \quad (10)$$

where $\Delta\omega_S = \omega_S - \omega$. We see from Eq. (10) that the two points are symmetrically located around the inflection point t_1 , which is a consequence of the expansion only up to the third order of $\gamma\delta n$ [Eq. (9)]. The phases ϕ_\pm of these two contributions are

$$\phi_\pm = \gamma\delta n(t_\pm) + \omega t_\pm. \quad (11)$$

If the above two contributions are required to be 180° out of phase, i. e., if it is required that

$$\phi_+ - \phi_- = \pi, \quad (12)$$

then the frequency ω should correspond to the first minimum of the spectrum. From Eq. (12), with the help of Eqs. (9)–(11), we can easily obtain

$$\left(\gamma \frac{d^3\delta n}{dt^3} \right)_1 = 0.36 (\Delta_1\omega_S)^3, \quad (13)$$

where $\Delta_1\omega_S$ is the frequency difference between the first maximum and first minimum of the spectrum at the Stokes side [see Fig. 2(a)]. Equation (13) readily gives $(\gamma d^3\delta n/dt^3)_1$ once $\Delta_1\omega_S$ is measured from the spectrum. To improve the accuracy of the measurement of $(\gamma d^3\delta n/dt^3)_1$ we may consider the l th minimum of the spectrum instead of the first one. If l is not too large, Eq. (9) still applies, and now Eq. (12) must be replaced with $\phi_+ - \phi_- = (2l - 1)\pi$. From this relation, with the help of Eqs. (9)–(11) one now gets

$$\left(\gamma \frac{d^3 \delta n}{dt^3} \right)_1 = 0.36 \frac{(\Delta_1 \omega_s)^3}{(2l-1)^2}, \quad (14)$$

where $\Delta_1 \omega_s$ is now the frequency difference between the first maximum and the l th minimum. From Eqs. (13) and (14) we readily obtain

$$\Delta_1 \omega_s = \Delta_1 \omega_s (2l-1)^{2/3}, \quad (15)$$

which predicts the positions of the minima of the spectrum as long as the third-order expansion given by Eq. (9) applies. From Eqs. (13)–(15) we immediately get the corresponding expressions for the anti-Stokes side by substituting the subscript 2 for the subscript 1 and ω_{as} for ω_s .

To calculate $\gamma \delta n_1$, we may now assume that the power expansion (9) provides for an accurate description of $\gamma \delta n(t)$ from the inflection point to the peak value. It can easily be verified, for example, that this is true for any Gaussian or Lorentzian pulse shape, the accuracy being better than 3%. Therefore we may now set the condition that the maximum value of $\gamma \delta n$ as obtained from Eq. (9) be equal to $\gamma \delta n_p$, whose value has already been calculated [Eq. (7)]. In this way, with the help of Eq. (13), we can easily obtain

$$\gamma \delta n_1 = \left[1 - \frac{0.5}{2m-1} \left(\frac{\omega_s}{\Delta_1 \omega_s} \right)^{3/2} \right] (2m-1)\pi. \quad (16)$$

A similar expression can be derived, in the usual way, for $\gamma \delta n_2$. We may therefore note that, if $(\omega_s/\Delta_1 \omega_s) \neq (\omega_{as}/\Delta_1 \omega_{as})$, the heights of the two inflection points will be different.

IV. MOLECULAR ROCKING

Equations (3)–(16), which will be used in this and in the following sections, have been derived on the basis of the method of stationary phase and of simple power expansions of $\gamma \delta n$. No hypothesis has been made, up to now, on the functional relation between δn and the electric field amplitude $A(t)$. Such a relation will be considered in this section.

The experimental results obtained using a Q-switched laser pulse lasting a few or a few tens of nanoseconds appear to be well interpreted by assuming that the molecular orientational Kerr effect is the main mechanism to produce a nonlinear refractive index.¹ Only the size of the filament diameter does not agree with the theoretical expectations^{18,19} or, alternatively, the theoretical trapped power does not correspond to the experimental one.²⁰ In this case, δn is related to the electric field amplitude by the well-known equation⁴:

$$\tau \frac{d\delta n}{dt} + \delta n = n_2 A^2, \quad (17)$$

where τ is one-third of the Debye relaxation time. However, with laser pulses shorter than τ , the orientational Kerr effect should be almost quenched. This should be the case with picosecond laser pulses for most of the liquids used in our experiments. In this case, according to a model introduced by Starunov,²¹ a different physical mechanism involving "rocking" of molecules in the field of neighboring molecules has been previously considered⁹ as a possible source for δn . This mechanism is characterized by a relaxation time τ_1 considerably shorter than τ (by even more than one order of magnitude, according to the liquid), so that it can respond to a fast excitation. Starunov's model refers to a possible aspect of molecular movement in liquids, i.e., to elastic vibrations of linear molecules in the field of neighboring molecules. The model was introduced to give an interpretation of the far wing of the Rayleigh line. Roughly speaking, if the excitation pulses have a duration shorter than the lifetime of the molecules in the potential well, the motions of the molecules may be regarded as elastic vibrations. In this case, the nonlinear polarization is a consequence of small rotations $\delta\theta$ of each molecule about its equilibrium position, the rotations being driven by a torque proportional to the square field amplitude A^2 . To these rotations, induced by the laser intensity, it is referred to here as a stimulated rocking of molecules. During longer excitations, many transitions of the molecules may occur from one potential well to another, and there results a rotational diffusion, which gives rise to the molecular orientational Kerr effect. In this case, the nonlinear polarization is a consequence of the molecular orientation about the electric field, described by a Maxwell-Boltzmann distribution.¹

If $\delta\theta$ is the angle of deviation of the molecular axis from its equilibrium position θ , the motion of the molecule, under the influence of the linearly polarized electric field $E = \frac{1}{2} A e^{i(kz - \omega_0 t)} + c. c.$ of an ultrashort laser pulse, will then be described by the equation^{21,22}

$$I \frac{d^2 \delta\theta}{dt^2} + \xi \frac{d\delta\theta}{dt} + \mu \delta\theta = \frac{\alpha}{3} L^2 A^2 \sin\theta \cos\theta. \quad (18)$$

I is the moment of inertia of the molecule, ξ is a coefficient of internal friction, μ is the elastic constant, $\alpha = \alpha_3 - \alpha_1$ is the difference between the polarizabilities parallel and perpendicular to the molecular axis. L is a local-field correction factor which, in the simple case of a Lorentz cavity, takes the form $L = \frac{1}{3}(n_0^2 + 2)$, where n_0 is the linear index of refraction. The right-hand side of Eq. (18) represents the torque exerted by the electric field on the molecule. The particular expression of the torque suggests that a solution of the type

$$\delta\theta = c(t) \sin\theta \cos\theta \quad (19)$$

can be assumed for $\delta\theta$. By substitution of (19) in (18) one gets

$$I \frac{d^2c}{dt^2} + \xi \frac{dc}{dt} + \mu c = \frac{1}{2} \alpha L^2 A^2. \quad (20)$$

The nonlinear refractive index is now derived from the average nonlinear polarization along the field direction:

$$\delta P^{NL} = N \int \delta p^{NL} P(\Omega) d\Omega / \int P(\Omega) d\Omega. \quad (21)$$

Here

$$\delta p^{NL} = 2\alpha L E \sin\theta \cos\theta \delta\theta \quad (21')$$

is the induced dipole moment (along the field direction) which corresponds to an angular displacement $\delta\theta$, $P(\Omega) d\Omega$ is the probability of a molecule having its axis of symmetry in a solid-angle element $d\Omega$, making an angle θ with respect to the electric field, and N is the number of molecules per unit volume. It is now assumed $P(\Omega) = \text{const}$, i.e., a random orientation of the molecules. This assumption appears to be reasonable since, for a short light pulse, the molecules have no time to reach their Maxwell-Boltzmann distribution, corresponding to the optical field $A(t)$.¹ From Eq. (21) with the help of Eqs. (21') and (19) we then get

$$\begin{aligned} \delta P^{NL} &= 2N\alpha L E c(t) \int_0^\pi \sin^3\theta \cos^2\theta d\theta / \int_0^\pi \sin\theta d\theta \\ &= \frac{4}{15} N\alpha L E c(t). \end{aligned} \quad (22)$$

Since $L \delta P^{NL} = 2\epsilon_0 n_0 \delta n E$, the following expression is derived for δn :

$$\delta n = (2/15\epsilon_0 n_0) N\alpha L^2 c(t). \quad (23)$$

From Eq. (20), a differential equation is derived which gives a functional relation between δn and the field amplitude A :

$$\tau_2^2 \frac{d^2\delta n}{dt^2} + \tau_1 \frac{d\delta n}{dt} + \delta n = n_2 A^2, \quad (24)$$

where $\tau_2 = (I/\mu)^{1/2}$, $\tau_1 = \xi/\mu$, and $n_2 = L^4 N \alpha^2 / 15\epsilon_0 n_0 \mu$. It is worth comparing Eq. (24) with Eq. (17), which refers to the Kerr effect. The main formal difference is due to the presence of an inertial term in Eq. (24); however significant differences also exist between the coefficients n_2 and between τ and τ_1 . Namely, since for the Kerr effect^{1, 23} $(n_2)_{\text{Kerr}} = L_4 \alpha^2 N / 90\epsilon_0 n_0 kT$, we get $(n_2)_{\text{rocking}} / (n_2)_{\text{Kerr}} = 6kT/\mu$. For CS_2 , taking for μ the numerical value given in Ref. 24, we get $(n_2)_{\text{rocking}} / (n_2)_{\text{Kerr}} \approx 0.2$ at room temperature.

The most important difference occurs between

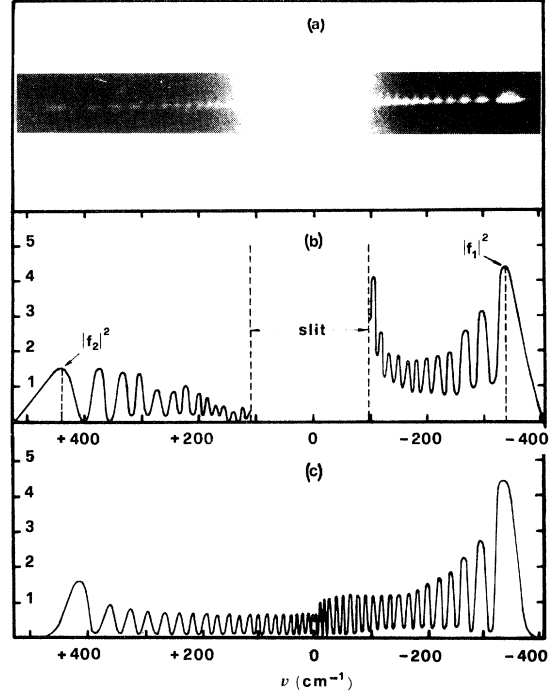


FIG. 3. (a) Picture of the typical spectrum of a filament. The central part of the picture is saturated by light entering the open slit of the spectrograph. (b) Intensity profile of the spectrum as recorded by means of a microdensitometer and corrected by taking into account the contrast factor of the film (Kodak 1N). (c) Intensity profile of the spectrum as obtained by computer, using the pulses represented in Fig. 4 for $\delta n(t)$ and the field amplitude $A(t)$. A numerical comparison between the spectra (b) and (c) is made in Table I.

τ and τ_1 . While τ is in the range of a few or a few tens of picoseconds,²⁵ τ_1 is in the range of a few tenths of picoseconds. Measurements of τ_1 had already been deduced from the extreme wing of the spontaneous Rayleigh line,²⁴ but, as pointed out in Ref. 9, Eq. (24), in connection with some of the relations derived in Sec. III, allows a measurement of τ_1 from the spectra of the filaments.

V. DISCUSSION AND NUMERICAL EXAMPLE

Following the theory developed in the previous sections, a numerical example is considered here. The purpose of this example is to show that many quantities of interest for the trapping phenomenon can be deduced from the spectra. Namely, we can obtain the time behavior of the nonlinear refractive index δn and of the field intensity A^2 in the filament, as well as the relaxation time τ_1 .

Let us consider the spectrum indicated in Fig. 3(a). In order to obtain precise numerical evaluations, the intensity profile of the spectrum has been recorded by means of a microdensitometer, and by using the characteristic curve of the film

(Kodak 1N). This curve has been checked with picosecond excitation and found to be in agreement with the nominal one. By subtracting the extended background due to the widely open slit of the spectrograph, we get the intensity profile of Fig. 3(b), which contains enough details for our purpose.

An approximate time behavior of $\gamma\delta n(t)$ can now be obtained on the basis of the third-order expansion given by Eq. (9). The quantities $\gamma\delta n_1$, ω_s , and $(\gamma d^3\delta n/dt^3)_1$ appearing in the equation are readily obtained from the spectrum of Fig. 3(b) with the help of Eqs. (19) and (16). Once Eq. (9) is applied to both the Stokes and anti-Stokes sides of the spectrum, the curve shown in Fig. 4 is obtained for $\gamma\delta n(t)$. It is worth noting that the resulting pulse is not symmetrical. In fact, we get $\delta n_1/\delta n_p = 0.536$ and $\delta n_2/\delta n_p = 0.59$, and the distances of the inflection points from the peak are 1.4 and 0.95 psec, respectively.

We may now ask how well the third-order expansion (9) agrees with the experimental results. To this end, a plot is shown in Fig. 5 of the observed position of the minima of the spectrum versus the parameter $(2l-1)^{2/3}$, where l is the order of the minima. According to Eq. (15), which is based on (9), the plot should give a straight line. We see that Eq. (15) is very well followed up to approximately the ninth minimum (points B and C in Fig. 5) for both the Stokes and anti-Stokes sides of the spectrum. Since the ninth minimum corresponds to a broadening which is ≈ 0.4 times the extension of the spectrum, it follows that the third-order expansion (9) represents satisfactorily the time behavior of δn between points B' and B'' and points C' and C'' of Fig. 4. Since, however, B' and C' lie very near the peak of the pulse, one can also assume that Eq. (9) gives a good description of $\gamma\delta n$ for the entire interval of time between points B'' and C''. From the present theory, no information can be obtained for the tails of the pulse, i.e., beyond points B'' and C''.

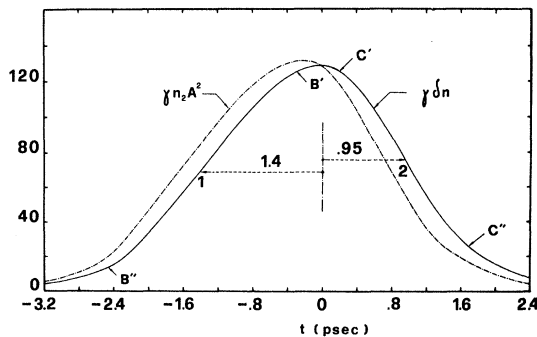


FIG. 4. Temporal behavior of the nonlinear refractive index $\delta n(t)$ and of the field intensity $A^2(t)$, as derived in the text from the experimental spectrum of the filament represented in Fig. 3.

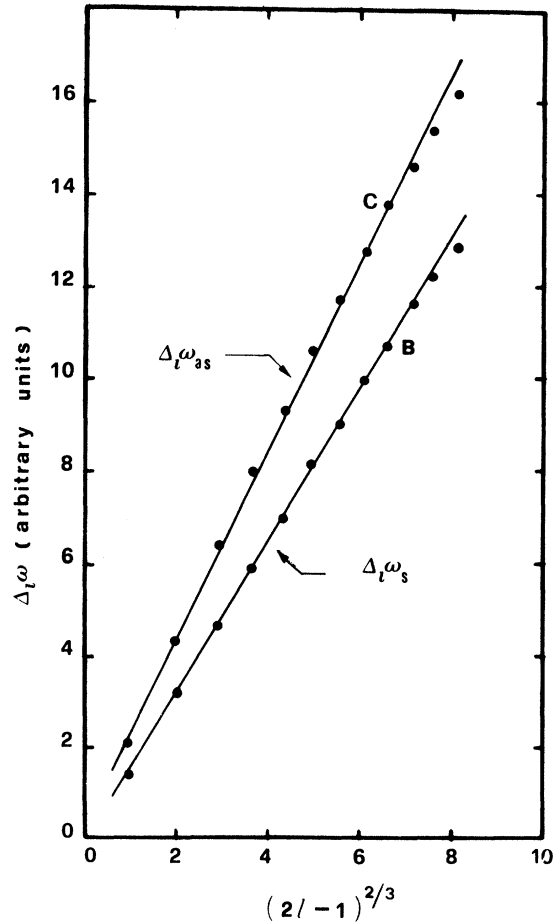


FIG. 5. Experimental plot of the position of the minima of the spectrum in Fig. 3(b) (dots) versus the parameter $(2l-1)^{2/3}$. The quantity $\Delta_l\omega_s$ is the angular-frequency separation between the highest maximum of the Stokes side and the l th minimum. The quantity $\Delta_l\omega_{as}$ has the same meaning for the anti-Stokes side of the spectrum. The straight lines in the figure are the theoretical predictions [Eq. (15)] on the basis of a third-order expansion for $\gamma\delta n(t)$.

Therefore, exponential tails matching the slope of $\gamma\delta n$ at B' and C' have been arbitrarily assumed in Fig. 4.

Since $\gamma\delta n(t)$ is now known, the optical pulse $A^2(t)$ can be obtained from Eq. (24) once τ_1 and τ_2 are known. The quantity τ_1 can also be directly obtained from the spectrum of Fig. 3(b). Although the resulting expression for τ_1 has already been given in a previous work,⁹ the derivation of this expression is here reported for the sake of completeness. Considering Eq. (24) at the two points t_1 and t_2 [Fig. 2(b)] where $d^2\delta n/dt^2=0$, taking the ratio of the two expressions, and using Eqs. (3) and (7) with $m \gg 1$, we have

$$\frac{\tau_1(|\nu_s|/m)\delta n_b + \delta n_1}{-\tau_1(|\nu_{as}|/m)\delta n_p + \delta n_2} = \frac{A_1^2}{A_2^2}, \quad (25)$$

where A_1^2 and A_2^2 are the square field amplitudes at the times t_1 and t_2 , respectively. Using Eqs. (8) and (13) for the right-hand side, Eq. (25) becomes

$$\frac{\tau_1(|\nu_S|/m) + (\delta n_1/\delta n_p)}{-\tau_1(|\nu_{aS}|/m) + (\delta n_2/\delta n_p)} = \frac{|f_1|^2}{|f_2|^2} \frac{\Delta_1 \nu_S^2}{\Delta_1 \nu_{aS}^2}, \quad (26)$$

where $|f_1|^2$ and $|f_2|^2$ are shown in Fig. 3(b). Equation (26) gives the value of τ_1 , since all the other quantities can be measured from the spectra. For the spectra of Fig. 3(b), Eq. (26) gives $\tau_1 \approx 0.25$ psec, in agreement with the numerical results reported under Ref. 9. Unfortunately, the theory presented here does not appear to be able to give a similarly simple expression for τ_2 . If, however, we assume for τ_2 a value of ≈ 0.21 psec, as estimated from the Rayleigh-wing scattering experiments,²⁴ we see from Eq. (24) that the term $\tau_2^2 \times d^2 \delta n/dt^2$ gives only a correction of a few percent around the peak of $\gamma \delta n(t)$. The optical pulse $A^2(t)$ can therefore be obtained from Eq. (24) simplified, to a first approximation, assuming that $\tau_2 = 0$. The pulse is shown in Fig. 4. The pulse width at half-intensity is 2.5 psec. Since the input pulses have a duration of ≈ 5 psec, a pulse shortening by a factor 2 seems to occur. One cannot, however, exclude the possibility that this time shortening is only apparent. Indeed, the measurement of the pulse width of the input pulses has been made by the usual two-photon fluorescence technique.²⁶ This gives an average value of the pulse width which might change by a factor 2 from one pulse to another of the mode-locked train. However, since pulses ≈ 2 psec wide have always been measured in the filaments, even by using input pulses which are 10 or 20 psec wide (on the average),¹¹ it is more likely that a real-time shortening occurs and is due to the self-focusing process.⁵ An asymmetry is also apparent in the shape of the pulse of Fig. 4, the trailing edge being steeper than the leading edge. This may be due to a self-steepening process²⁷ over the traveling distance z of the filament. An alternative explanation is that the input pulses are in themselves asymmetrical.

TABLE I. Numerical comparison between the experimental spectrum [Fig. 3(b)] and the computed spectrum [Fig. 3(c)].

Physical quantity	Experimental results	Computer results
ν_S (cm ⁻¹)	-340	-336
ν_{aS} (cm ⁻¹)	444	412
ν_{aS}/ν_S	1.3	1.22
$ f_1 ^2/ f_2 ^2$	2.9	2.75
$\Delta_1 \nu_S$ (cm ⁻¹)	29.6	27.4
$\Delta_1 \nu_{aS}$	42.5	36.3
m	20	20

The considerations so far presented make it possible to measure the absolute value of $\gamma \delta n(t)$ and $\gamma n_2 A^2(t)$. If $\gamma = \omega_0 z/c$ (i.e., the traveling distance z of the filament) were known, we could immediately obtain the absolute value of $\delta n(t)$. Although the distance z can, in principle, be obtained with the pin-hole technique suggested by Denariez and Taran,¹⁷ an alternative way is to obtain an approximate absolute value of δn from measurements of the filament diameter. Indeed, by equating the critical angle for trapping to the diffraction angle of the trapped beam we get¹

$$(2\delta n/n)^{1/2} = (1.22/2.88)\lambda/d, \quad (27)$$

where d is the filament diameter. Since the measured diameter of our filaments is $\approx 5\mu$ (the measurement being made with a resolving power of $\approx 1.3\mu$), we get from Eq. (27) approximately $\delta n_p \approx 2.64 \times 10^{-3}$. This value gives a traveling distance $z = c\gamma/\omega_0 \approx 0.54$ cm for the filament, in agreement with the values found in Ref. 17. The peak value of $n_2 A^2$ is therefore $\approx 1.7 \times 10^{-3}$, and assuming for CS₂, $(n_2)_{\text{rocking}}/(n_2)_{\text{Kerr}} \approx 0.2$, a maximum field amplitude of $\sim 10^7$ V/cm is arrived at. Integration of the pulse intensity over a time width of 2.5 psec and a cross section of $\approx 5\mu$ diam gives an energy of about 1 erg for the filament. This is in agreement with the measurement of filament energy made photographically by means of near-field pictures of the filaments, once the sensitivity of the film is known.

The analysis carried out up to now has been based on the method of stationary phase. By this method a number of quantities directly deducible from the spectra have been deduced which, inserted in the expansion (9), enable us to know the time behavior of δn . Then, using a functional relation between δn and A^2 based on Starunov's model, we can also obtain the pulse $A^2(t)$. In order to check the self-consistency of this procedure, $\gamma \delta n(t)$ and $A(t)$, obtained in this way, were put in the integral (1), which was then calculated by computer. The resulting spectral power density $|f|^2$ is represented in Fig. 3(c) and must be compared with the experimental one shown in Fig. 3(b). The comparison, which is made in Table I, indicates that the computed spectrum agrees well the experimental one and therefore indicates that the pulses $\gamma \delta n(t)$ and $A^2(t)$ previously derived accurately describe the physical process. In particular, the computed spectrum contains a number of minima m which are the same for both the Stokes and the anti-Stokes sides, and $m = 20$ is in agreement with the corresponding experimental value.

VI. CONCLUSIONS

The spectral properties of trapped filaments of

light have been extensively studied. By means of the method of stationary phase an important piece of information on the trapping phenomenon, namely, the time behavior of the nonlinear refractive index has been obtained. Furthermore, by making use of Starunov's model, the time behavior, the pulse intensity in the filaments, and the value of the relaxation time τ_1 of the nonlinear refractive index have also been derived. In particular, the measurement of τ_1 , which is consistently in the range of a few tenths of a picosecond, is a strong indication that a "molecular rocking" is the main mechanism for trapping with picosecond excitation. The self-consistency of the method employed has been checked by using the pulses $\gamma\delta n(t)$ and $A(t)$ previously obtained to calculate, by computer, the corresponding spectral power density to be compared with the

experimental one. The resulting high degree of agreement indicates that the pulses have been derived with close approximation.

It may be concluded that useful pieces of information on important physical parameters of the trapping phenomenon can be derived by combining clean reproducible experimental results obtained with picosecond excitation with a rather simple, yet powerful, method of analysis. In this way, a deeper insight into the whole dynamics of the trapping phenomenon becomes possible.

ACKNOWLEDGMENTS

We wish to thank S. Brughera and M. Scattorin for their very helpful technical assistance, and Dr. A. Ghirardi and Dr. S. Osnaghi of the CISE Laboratories for computer calculations.

*Work supported by the Italian Consiglio Nazionale delle Ricerche, Milano, Italy.

¹R. G. Brewer, J. R. Lifshitz, E. Garmire, R. Y. Chiao, and C. H. Townes, *Phys. Rev.* **166**, 326 (1968).

²H. P. H. Grieneisen and C. A. Sacchi, *Bull. Am. Phys. Soc.* **12**, 686 (1967); (J. R. Lifshitz should be included as an author of that paper, since his name was accidentally omitted in publication); R. G. Brewer, *Phys. Rev. Letters* **19**, 8 (1967).

³F. Shimizu, *Phys. Rev. Letters* **19**, 1097 (1967).

⁴T. K. Gustafson, J. P. Taran, H. A. Haus, J. R. Lifshitz, and P. L. Kelley, *Phys. Rev.* **177**, 306 (1969).

⁵J. H. Marburger and W. G. Wagner, *IEEE J. Quantum Electron.* **QE-3**, 415 (1967).

⁶A. C. Cheung, D. M. Rank, R. Y. Chiao, and C. H. Townes, *Phys. Rev. Letters* **20**, 786 (1968).

⁷J. R. Lifshitz and H. P. H. Grieneisen, *Appl. Phys. Letters* **13**, 245 (1968).

⁸R. G. Brewer and C. H. Lee, *Phys. Rev. Letters* **21**, 267 (1968).

⁹R. Polloni, C. A. Sacchi, and O. Svelto, *Phys. Rev. Letters* **23**, 690 (1969).

¹⁰G. Soncini and O. Svelto, *IEEE J. Quantum Electron.* **QE-4**, 422 (1968).

¹¹R. Cubeddu, R. Polloni, C. A. Sacchi, and O. Svelto, *IEEE J. Quantum Electron.* **QE-5**, 470 (1969).

¹²R. Polloni, S. Riva, G. Soncini, and O. Svelto, *High Frequency Generation and Amplification* (Cornell U. P., Ithaca, N. Y., 1967), pp. 31-37.

¹³M. Maier, W. Kaiser, and J. A. Giordmaine,

Phys. Rev. Letters **17**, 1275 (1966); M. Maier, *Phys. Rev.* **166**, 113 (1968).

¹⁴E. Garmire and C. H. Townes, *Appl. Phys. Letters* **5**, 84 (1964).

¹⁵N. H. Kroll, *J. Appl. Phys.* **36**, 34 (1965).

¹⁶E. T. Copson, *Asymptotic Expansions* (Cambridge U. P., Cambridge, England, 1965), Chap. IV.

¹⁷M. M. Denariez-Roberge and J. P. E. Taran, *Appl. Phys. Letters* **14**, 205 (1969).

¹⁸T. K. Gustafson, P. L. Kelley, R. Y. Chiao, and R. G. Brewer, *Appl. Phys. Letters* **12**, 165 (1968).

¹⁹J. Marburger, L. Huff, J. D. Reichert, and W. G. Wagner, *Phys. Rev.* **184**, 255 (1969).

²⁰A. H. Piekara, *Appl. Phys. Letters* **13**, 225 (1968).

²¹V. S. Starunov, *Opt. i Spektroskopiya* **18**, 300 (1965) [*Opt. Spectry, (USSR)* **18**, 165 (1965)].

²²O. Rahn, M. Maier, and W. Kaiser, *Opt. Commun.* **1**, 109 (1969).

²³N. Bloembergen and P. Lallemand, *Phys. Rev. Letters* **16**, 81 (1966).

²⁴I. L. Fabelinskii and V. S. Starunov, *Appl. Opt.* **6**, 1793 (1967).

²⁵M. F. Vuks and A. A. Atakhodzaev, *Dokl. Akad. Nauk SSSR* **109**, 926 (1956) [*Soviet Phys. Doklady* **1**, 496 (1956)].

²⁶J. A. Giordmaine, P. M. Rentzepis, S. L. Shapiro, and K. W. Wecht, *Appl. Phys. Letters* **11**, 216 (1967).

²⁷F. De Martini, C. H. Townes, T. K. Gustafson, and P. L. Kelley, *Phys. Rev.* **164**, 312 (1967).

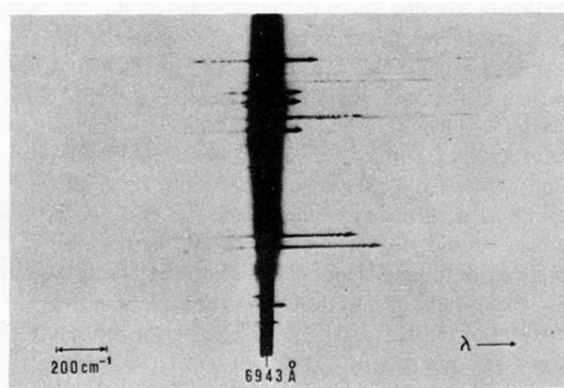


FIG. 1. Typical regular spectra due to self-phase modulation as obtained with picosecond excitation.

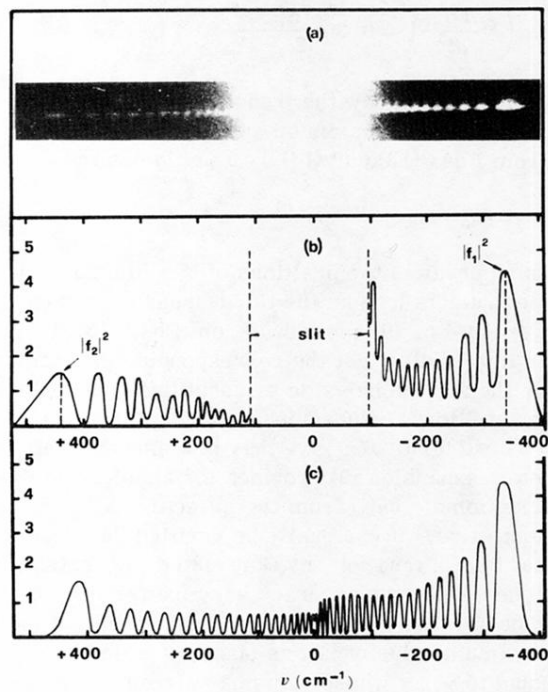


FIG. 3. (a) Picture of the typical spectrum of a filament. The central part of the picture is saturated by light entering the open slit of the spectrograph. (b) Intensity profile of the spectrum as recorded by means of a microdensitometer and corrected by taking into account the contrast factor of the film (Kodak 1N). (c) Intensity profile of the spectrum as obtained by computer, using the pulses represented in Fig. 4 for $\delta n(t)$ and the field amplitude $A(t)$. A numerical comparison between the spectra (b) and (c) is made in Table I.